IEEE/CSC & ESAS SUPERCONDUCTIVITY NEWS FORUM (global edition), January 2016.
EUCAS 2015 preprint 2M-WT-O15. Submitted to *IEEE Trans. Appl. Supercond.* for possible publication.

Characterization of CICC superconductor wires

Maria S. Commisso, Eric Maire, Jean-Yves Buffiere and Daniel Ciazynski

***Abstract*—The Nb_3Sn cable in conduit conductors (CICCs) have a multi-stage twisted configuration. The inner structure of CICC such as the twist pitch and void fraction have a substantial impact on the superconductive cable performances. X-ray tomography is a powerful non-destructive technique which can provide 3D images of strands configuration. Therefore, this technique is used to determine the internal structure of the cables which in turn can be used to verify the cabling process and even further for modelling purposes. Additionally, scanning electron microscopy (SEM) analysis has been carried out to show the interaction between strands and to characterize the filaments of superconductive compound. Through an energy-dispersive X-ray spectroscopy (EDX) analysis, a chemical characterization of the superconductive filaments was performed. It was found that the trajectory of some strands was irregular and different to the one defined during cabling. Contacts between strands produces detachments between the central zone and the outer ring of pure copper. Regarding the superconductive filaments, the solid state reaction performed to obtain the superconductive compound was not fully completed and an inner central core composed of pure Nb was obtained in several filaments. Also, a tendency of the Nb filaments to bridge together could be observed and some cracks were seen, specially in those with an inner central core of pure Nb.**

I. Introduction

In terms of electric and magnetic stability Nb_3Sn cables are superior to NbTi cables because of their superior primary superconducting properties (upper critical field and critical temperature) [1], [2]. However, the Nb_3Sn superconductor compound is sensitive to strain [3]. Therefore, the performance of the superconducting properties of these cables are forcedly affected by the internal stresses and strains resulting from the manufacturing process.

The Nb_3Sn cable in conduit conductors (CICCs) have a multi-stage twisted configuration. The inner structure of CICC such as the twist pitch and void fraction have a substantial impact on CICC performance [4], [5]. Additionally, the strands are inserted into a stainless steel jacket to obtain the final cable. Due to the differential thermal contraction between materials, the change of temperature from heat treatment to cryogenic operational temperature produces contraction of the strands in the axial direction and bending which is greatly affected by the cable twist pattern [6]. The strand-to-strand contacts also transfer loads into the strands. These bending and contact loads generate periodic strain variations along the Nb_3Sn filaments, which in turn determine the degree of change in the critical current and the possible occurrence of filament breakage [6].

M.S. Commisso, E. Maire and J-Y. Buffiere are with the University of Lyon, INSA-Lyon, MATEIS, CNRS UMR5510, F-69621 Villeurbanne, France e-mail: maria-soledad.commisso@insa.lyon.fr

D. Ciazynski is with Association Euratom-CEA, CEA/DSM/DRFC, CEA/Cadarache, F-13108, Saint-Paullez- Durance, France.

Manuscript received September 8, 2015.

Therefore, the selection of the twist pitch length is of great importance in the performance of the superconductive cables and specially in those strain-sensitive superconductors like Nb_3Sn [6].

In several works, the cable twisting have been modelled [7]–[11]. Furthermore, the spatial structure of a superconductor cable made of multi-stage twisted strands is necessary for accurate simulation of void statistics, strain effect, AC loss current distribution, etc [7].

X-ray tomography is a non-destructive technique which can provide 3D images of complex microstructures. However, tomography scans of CICC samples is seriously challenging due to the high effective atomic number of the outer layer. Therefore, high-energy, high-intensity and small focus spot X-ray source is needed.

The aim of this work is to characterize the actual 3D inner structure of Nb_3Sn cable in conduit conductors by using X-ray microtomography. Also, scanning electron microscopy has been carried out to characterize the interaction between strands and to observe the filaments of Nb_3Sn at high spatial resolution.

II. Material and Methods

Three CICC cables were studied. The multi-stage configuration is built up by twisting sub-elements. In the studied cases, the cables have three stages of twist and were built up from a 3 x 3 x 5 combination of sub-elements with different twist pitches. The multifilament Nb_3Sn-based composite strand has been bundled together with copper strands in different ratios. In table I the main characteristics, such as the relation between the superconductive strands (SCS) and the Copper ones (CuS), the fabrication twist pitch (TP) the void fraction (VF) and the external diameter of the cable (ϕ_{ext}) of each one of them is detailed.

TABLE I
Cables characteristics: (1) SCS:CuS ratio, (2) manufacturing twist pitch, (3) void fraction and (4) cable external diameter.

samples	**ratio**$^{(1)}$	**TP** $(mm)^{(2)}$	**VF**$^{(3)}$	ϕ_{ext} $(mm)^{(4)}$
N05	2	45/85/125	25%	7.05
N22	0.5	45/85/125	32%	7.35
N25	2	35/65/110	32%	7.35

The cables were composed of 45 strands with a diameter of $0.8\ mm$. The internal tin fabrication route was used to produce the Nb_3Sn filaments, a Ta anti-diffusion barrier was used and a Copper external shell can be found around the filament region.

Scanning electron microscopy and tomography scans were used to analyze the microstructure of the cables. The tomograph used for imaging was a VtomeX system manufactured

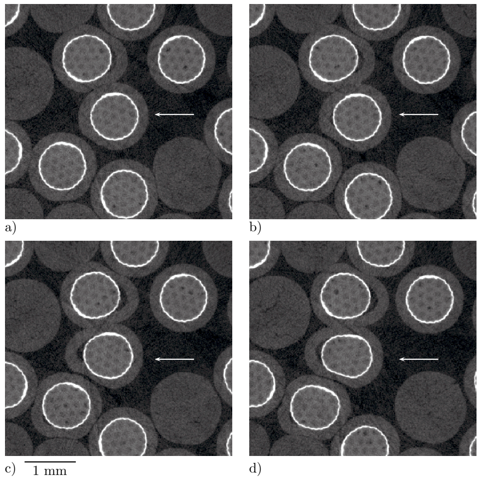

Fig. 1. X-ray tomography images of four transversal areas of N25 cable taken with a voxel size of $4\mu m$. Arrows indicate a strand at different cross sections along the cable axis and how the contact with other strands produces an interfacial decohesion.

by Phoenix X-Rays (for more detailed information see [12]). The tomograph was operated with a 150kV acceleration voltage using a tungsten transmission target with a $60\mu A$ current. The incident X-ray beam was filtered with a copper plate of $0.5mm$ thickness and a time per scan of $\sim10min$ was required. X-ray tomography scans with a voxel size of $4\mu m$ and $12\mu m$ were acquired. To determine the twist pitch of the cables, successive acquisitions were performed by physically displacing the sample parallel to its axis. The scans presented an overlapping region that allowed us to merge them. The scanning parameters were selected to obtain the best quality image possible while keeping the voxel size as large as possible to reduce the amount of successive scans. The selected size for determining the TP was $12\mu m$. The reconstruction algorithm used was a standard filtered back projection implemented in the tomograph.

To further observe the contact interactions between strands and to characterize the Nb_3Sn filaments, scanning electron microscope (SEM) analysis was performed in samples prepared by conventional method: manual polishing plus vibrational polishing as recommended in [13].

III. RESULTS

The tomograph scan performed with a voxel size of $4\mu m$ allowed us to observe the contact interaction between superconductor and Copper strands. Figure 1 displays images obtained by X-ray tomography in the N25 cable at different heights along the sample axis. Interfacial decohesion between the outer core of Cu and the inner region of superconductor filaments can be seen (arrows on figure 1) and seems to be caused by the contact interaction between strands.

Figure 2 presents two images obtained with secondary electron detectors where it can be seen that the contact between strands deformed the outer surfaces of the strands and seems to be associated with the detachment between the outer core and the inner region in the SCS.

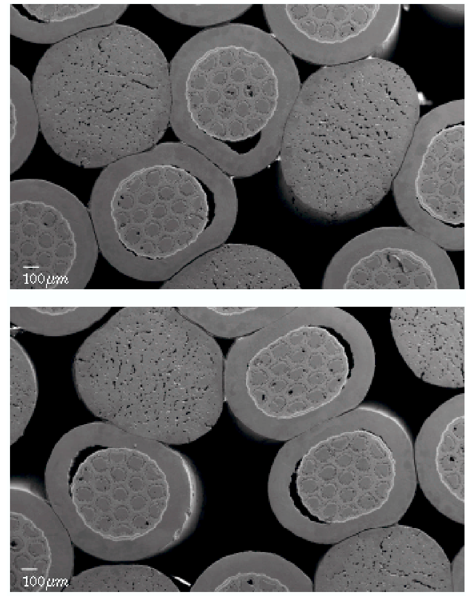

Fig. 2. SEM image of contact interaction between SCS and CuS obtained with secondary electron detectors.

Additional analysis with SEM was carried out with backscattered electron (BSE) detector. The intensity of BSE signal is strongly related to the atomic number, therefore it can provide information about the different chemical compounds in the strand. Figure 3a) shows a BSE image of a superconductor strand. An inner filament region separated by a Ta barrier (white layer) from an external Copper zone can be distinguished. Figure 3b) exhibits a magnified image of the circled region shown on figure 3a). It can be seen that there are 4 layers of superconductor filaments surrounding a central area of plain copper (darker grey).

There is a tendency of the filaments to bridge together as can be seen in image 3c). This can be due to the fact that in the internal tin fabrication method, the Nb filaments are usually closely spaced to increase the volume fraction available for conversion to Nb_3Sn [13]. However, this has the disadvantage of filament agglomeration after reaction because the molar volume of the Nb_3Sn compound is larger than the molar volume of Nb [13].

Also, cracks can be observed in the filaments specially in those with an inner central core (figure 3c)).

Through an energy-dispersive X-ray spectroscopy (EDX) analysis, a chemical characterization of the filaments was performed. The stoichiometric composition is obtained along a line across filament diameter (see figure 4). There is a circular region of around $1\mu m$ of diameter in the center of the filament where the atomic composition of almost pure Nb was obtained. The internal tin fabrication method requires a diffusion of the Sn into Nb filaments to conduct a solid state reaction to finally obtain the Nb_3Sn compound. In several filaments, it seems that the solid state reaction was not completed leaving a Nb island in the center of the filament.

The X-ray tomograph images were segmented by defining a threshold to select the strands. Then a series of successive

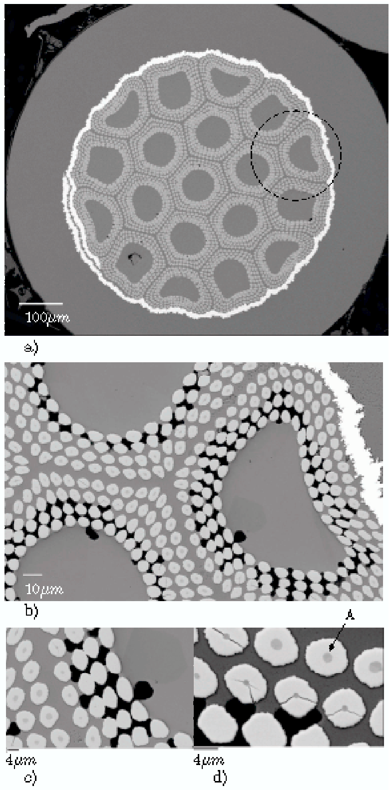

Fig. 3. SEM image of a SCS obtained by BSE at different magnification. Darker areas represent holes in the material (b, c and d). Cracks can be observed in the filaments (d). "A" indicates: Nb island.

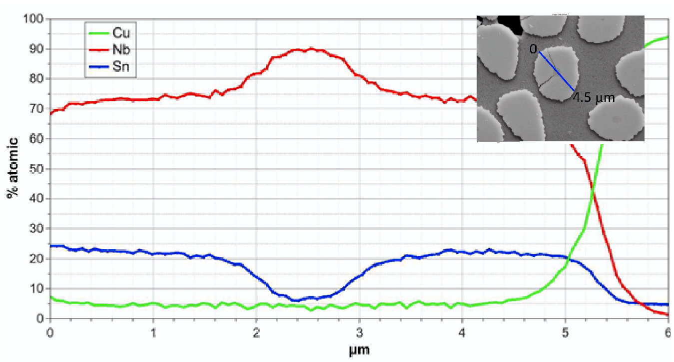

Fig. 4. Evolution of the chemical composition across a diameter of filament of Nb_3Sn obtained by EDX.

image processing steps were applied to the images to separate one strand from the others: close/open and dilate/erode processes. Finally a local thickness analysis was performed. An example of the resulting segmentation is shown in figure 5.

The twisting of the cable defines the displacement of each strand in the cable cross-section while shifting from one cross-section to another one. The centroid of each strand was defined by a position vector (r_i) in each cross section. For the whole set of cross sections, the position vector of each strand (r_i) can be fitted with a circled arc which in turn allows us to define a new origin (o_i). Therefore, the angle α_i can also be estimated (see figure 6). Finally the length of the cable corresponding to

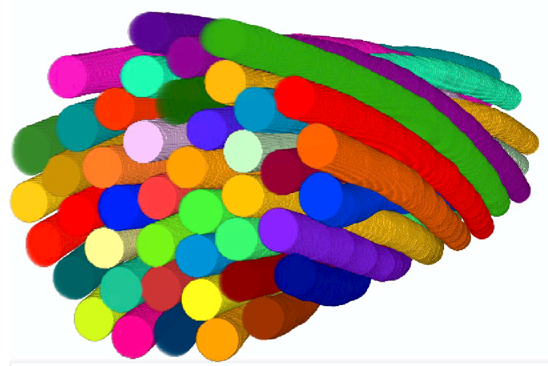

Fig. 5. 3D rendering of the strands observed in sample N25 from X-ray tomograph images.

a complete rotation, $\alpha_i = 360$, is defined as the Twist-Pitch of the strand (TP).

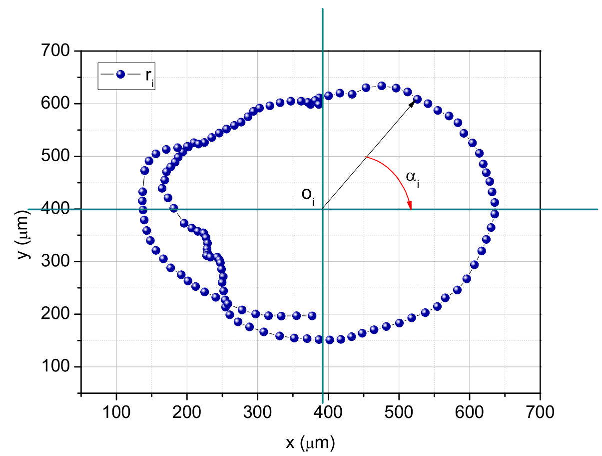

Fig. 6. Position vector r_i for a strand at different cross sections, along 147 mm of the cable N05.

The procedure was followed for each strand and the average TP was estimated for the three mentioned cables. Table II summarizes the results.

TABLE II
AVERAGE VALUE OF TP AND STANDARD DEVIATION FOR THE THREE ANALYZED SAMPLES.

samples	average **TP** (mm)	standard deviation (mm)
N05	126.5	± 14.6
N22	117.8	± 14.0
N25	99.8	± 15.3

The average value of TP is around 100 mm which is close to that recommended by [6] to avoid degradation of large CICCs. However, there were some irregularities in the pattern of the position vector of certain strands. Several strands presented a buckled trajectory. In figure 7, example cases of superconductive strands with that irregular pattern can be seen.

During the cooling step of the heat treatment, cables with small twist pitches can present periodic bending in different

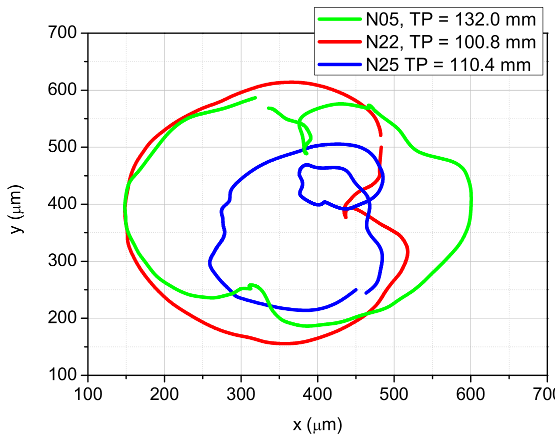

Fig. 7. Position of the center of mass of 3 superconductive strands at different cross sections in the three analyzed cables.

directions with a relatively short wavelength due to the lack of strand-to-strand support [6]. This can induce large bending strains and eventually buckling of single strands.

IV. Conclusion

The complex twisted structure of a superconducting cable was analyzed non destructively in 3D by the reconstruction of successive tomographic scans. The twist pattern was measured for the three analyzed cables obtaining an average twist around 100 mm. However, the trajectory of some strands presented some irregularities within the analyzed length. The tomograph scans also permitted the identification of strand-to-strand contact. These two parameters obtained with a non destructive technique can be a valuable tool for developing accurate models of the CICC cables.

The SEM analysis was useful to characterize the superconductive filaments and to further characterize the contact between strands. With an EDX analysis, it was seen that the solid state reaction was not fully completed obtaining a central core of pure Nb in some filaments. In addition, cracks were identified in the superconductive filaments.

Acknowledgment

Funding was provided by the French Agence Nationale de la Recherche through the cocascope project ANR-GUI-AAP-05.

References

[1] H. Kasahara, S. Torii, S. Akita, K. Uyeda, and et al., "Critical current of nb3sn superconductors for generators under cyclic mechanical load," *IEEE Trans. Magn*, vol. 30 (4), pp. 1927–1930, 1994.

[2] C. Fischer, "Investigation of the relationship between superconducting properties and nb3sn reaction conditions in powder in tube nb3sn conductors," Ph.D. dissertation, University of Wisconsin, 2002.

[3] N. Mitchell, "Summary, assessment and implications of the iter model coil test results," *Fusion Engineering and Design*, vol. 66–68, pp. 971–993, 2003.

[4] R. Mints and A. Rakhmanov, "The current-carrying capacity of twisted multifilamentary superconducting composites," *J. Phys, D: Appl. Phys.*, vol. 20, pp. 826–830, 1988.

[5] I. Tiseanu, L. Zani, T. Craciunescu, F. Cotorobai, C. Dobrea, and A. Sima, "Characterization of superconducting wires and cables by x-ray micro-tomography," *Supercond. Sci. Technol.*, vol. 88 (9-10), pp. 1613–1618, 2013.

[6] A. N. E. van Lanen and G. Rolando, "Optimization of iter nb3sn ciccs for coupling loss, transverse electromagnetic load and axial thermal contraction," *Supercond. Sci. Technol.*, vol. 25 (1), pp. 1–20, 2012.

[7] J. Feng, "A cable twisting model and its application in csic multi-stage cabling structure," *Fusion Engineering and Design*, vol. 84, pp. 2084–2092, 2009.

[8] Y. Li, X. Wang, Y. Gao, and Y. Zhou, "Modeling for mechanical response of cicc by hierarchical approach and abaqus simulation," *Fusion Engineering and Design*, vol. 88, pp. 2907–2917, 2013.

[9] M. Breschi, M. Ciotti, and P. Ribani, "Analysis of inductance coefficients in multi-strand cables: analysis, numerical and experimental results," *IEEE Trans. Appl. Super.*, vol. 15(3), pp. 3797–3807, 2005.

[10] M. Breschi and P. Ribani, "Electromagnetic modeling of the jacket in cable-in-conduit conductors," *IEEE Trans. Appl. Super.*, vol. 18, pp. 18–28, 2008.

[11] Y. Chen, "A comprehensive electromagnetic analysis of ac losses in large superconducting cables," Ph.D. dissertation, MIT, 1996.

[12] J.-Y. Buffiere, E. Maire, J. Adrien, J.-P. Masse, and E. Boller, "In situ experiments with x ray tomography: an attractive tool for experimental mechanics," *Exp. Mech.*, vol. 50 (2), pp. 289–305, 2010.

[13] M. Jewell, "The effect of strand architecture on the fracture propensity of nb3sn composite wires," Ph.D. dissertation, University of Wisconsin, 2008.